

RESEARCH

Open Access



The deception effect of FDA counteracting amplitude-comparison monopulse reconnaissance

Jiaang Ge* and Junwei Xie

*Correspondence:
gejiaang0313@163.com

Air and Missile Defense College,
Air Force Engineering University,
Xi'an 710051, Shaanxi, China

Abstract

Conventional phased array radar can direct the high-gain beam, resulting in high visibility under the reconnaissance system and even direct exposure to the enemy. As an amplitude-based direction-finding system, the amplitude monopulse system can recognize the traditional radar signals. However, there are still some issues with the countermeasures of the monopulse system, so it is necessary to find better styles of jamming. Since the beam of the frequency diverse array (FDA) signal at a certain angle varies with the range, we studied the deception effect of the FDA against the amplitude-comparison monopulse direction-finding system. By analyzing the established FDA-based direction-of-arrival location deception model against the amplitude-comparison monopulse system, we found that the introduction of the frequency increment might cause the FDA signals to deceit the monopulse system in principle. Then, to indicate the superiority of our deception method, we obtain the instantaneous signal-to-noise ratio, Cramér–Rao lower bound, root-means-square error, and variation. Numerical simulation results demonstrate that the FDA can generate deceptive signals to counteract the amplitude-comparison monopulse direction-finding system.

Keywords: Frequency diverse array (FDA), Direction-of-arrival (DOA), Location deception, Amplitude-comparison monopulse

1 Introduction

1.1 Background

Since its introduction in the last century, the phased array radar (PAR) has been extensively developed. The conventional PAR can steer the high-gain beam that can point in all directions, which means that the PAR has a flexible space detection capability. However, the high-gain beam also means high visibility for the reconnaissance system. Moreover, the high visibility may cause radar safety problems, and in severe cases, it may even damage the radar. Consequently, several techniques have been proposed to address these issues, with the main ones focusing on reducing visibility and improving the low probability of interception (LPI) [1–3]. However, it can be learned that the beam of PAR in a given angle is fixed for all ranges [4–8]; this means that the PAR may still be located by the amplitude method reconnaissance system in theory.

The amplitude monopulse direction-finding system is a standard amplitude method reconnaissance system. Recently, three countermeasures have been put in place for the monopulse system: (1) Incoherent jamming [9–11]: two or more jammers within the angular resolution unit of the monopulse radar are used for jamming, and since the jamming signals are incoherent, the incoherent jammer does not require the phases of the jamming signals. However, the deception angle is within the connection of jamming sources, meaning that the caused jamming error can be relatively small. (2) Cross-polarization jamming [12–14]: the radar receiving antenna has a fixed angle deviation from the cross-polarization jamming signals, inducing the radar angle tracking error. However, the cross-polarization jamming signals must be completely orthogonal to the main polarization signals, and the power of the jamming signals must be relatively high. (3) Cross-eye jamming [15–17]: reverse cross-eye jamming is an effective style of jamming against monopulse radar at this time; however, specific problems remain, such as the strict tolerance of system parameters and the requirement for a high signal-to-interference ratio. Therefore, it is urgently necessary to find better styles of jamming.

The frequency diverse array (FDA) is considered a feasible array solution to this problem. While compared with the phased array (PA), the FDA introduces small frequency increments between the array elements, forming a range-angle-dependent beampattern in the far-field [18]. Currently, FDA research focuses on beamforming [19, 20], angle-range joint estimation [21–23], FDA-MIMO [24, 25], and so on. The FDA also has a moral application prospect in electronic countermeasures (ECMS), and some researchers are concentrating on the FDA's superiority in radio frequency (RF) stealth. Thus, Wang [26] and Xiong et al. [27] propose LPI beamforming for the FDA radar and FDA-MIMO radar, respectively. Another method to realize RF stealth is location deception; thus, Ge et al. [28] proposes a cognitive active anti-jamming method based on the FDA phase center. Besides, several deception methods based on the FDA are proposed for some reconnaissance systems, and the current research mainly focuses on the interferometer [29–31] and the sum and difference beam reconnaissance [32].

1.2 Methods and contributions

However, since the beam of the FDA signal at a fixed angle varies according to the range, the FDA may also have a deception effect on the amplitude-comparison monopulse system. Therefore, we investigated the deception effect of the FDA to counteract the amplitude-comparison monopulse direction-finding system. The main works in this paper are listed as follows:

- (1) The deception model for the FDA against the amplitude-comparison monopulse reconnaissance is proposed. By analyzing the signal models of the FDA radar and the amplitude-comparison monopulse direction-finding system, we can see that the FDA signal received by the direction-finding system is not following the direction-finding principle of the amplitude-comparison monopulse, and thus, the deception model is established.
- (2) The deception effect in the non-noise environment is studied. We find that multiple parameters influence the deception effect through the DOA location deception model. Therefore, by comparing the three given FDA structures with different

frequency increment sequences with the PA, we analyze the influence of distance and frequency on the deception effect. Moreover, considering the time-dependent beampattern, the influence of the signal propagation time is also analyzed.

- (3) The deception effect in the noise environment is studied. Considering the range-angle-time-dependent beampattern of the FDA, we find that the FDA signal has the SNR variable with time in the constant noise environment. Therefore, the ISNR is derived and based on which the CRLB is also deduced. Furthermore, to signify the superiority of our deception method, the RMSE and Var are also derived.

The rest of this paper is organized as follows. Section 2 introduces and analyzes the signal model of the FDA and the amplitude-comparison monopulse system. Section 3 proposes the deception model of the amplitude-comparison monopulse direction-finding system based on the FDA. In addition, the ISNR, RMSE, Var, and CRLB are also derived, and then, the simulation results are given in Sect. 4. Finally, Sect. 5 draws the conclusions.

2 Signal model of FDA and amplitude-comparison monopulse

2.1 Signal model of FDA radar

As Fig. 1 illustrates, the Q -element linear FDA with the fixed element spacing d has different element radiation frequency f_q , that is

$$f_q = f_0 + \Delta f_q \quad (1)$$

where f_0 denotes the carrier frequency, and Δf_q denotes the frequency increment of the element q . Besides, let $\Delta f_1 = 0$, then $f_1 = f_0$.

Considering the XOZ plane as Fig. 1 shows, and supposing the far-field target is at (θ, R) , then the radiated signal from the element q to the target can be represented as

$$S_{tq}(t) = \exp [j2\pi f_q(t - R_q/c)] \quad (2)$$

where $c = 3 \times 10^8$ m/s denotes the speed of light and $R_q \approx R - (q - 1)d \sin \theta$ is the range to the element q . Then, we can know the synthesized signals at the given target are

$$E_{\text{FDA}} = \sum_{q=1}^Q A_q S_{tq}(t) = \sum_{q=1}^Q A_q \exp [j2\pi f_q(t - R_q/c)] \quad (3)$$

with A_q being the signal radiation amplitude of the q th element. And (3) can be further approximately expanded as

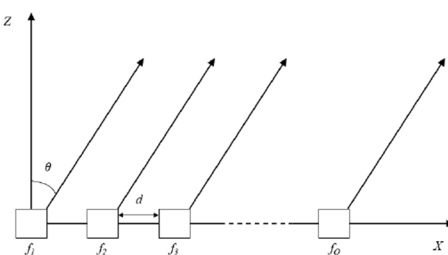


Fig. 1 Q-element linear FDA

$$\begin{aligned}
E_{\text{FDA}} &\approx \sum_{q=1}^Q A_q \exp \left[j2\pi (f_0 + \Delta f_q) \left(t - \frac{R - (q-1)d \sin \theta}{c} \right) \right] \\
&= \exp \left[j2\pi f_0 \left(t - \frac{R}{c} \right) \right] \sum_{q=1}^Q A_q \exp \left[j2\pi \left(\frac{f_0 (q-1)d \sin \theta}{c} + \Delta f_q t - \Delta f_q \frac{R}{c} + \Delta f_q \frac{(q-1)d \sin \theta}{c} \right) \right]
\end{aligned} \tag{4}$$

Supposing $A_q = A = 1$ and $\Delta f_q \ll f_0$, then (4) can be approximately rewritten as

$$\begin{aligned}
E_{\text{FDA}} &\approx \exp \left[j2\pi f_0 \left(t - \frac{R}{c} \right) \right] \sum_{q=1}^Q \exp \left[j2\pi \left(\frac{f_0 (q-1)d \sin \theta}{c} + \Delta f_q t - \Delta f_q \frac{R}{c} \right) \right] \\
&= A_{\text{BP_FDA}} e^{j\Psi_{\text{FDA}}}
\end{aligned} \tag{5}$$

where $A_{\text{BP_FDA}} = |E_{\text{FDA}}|$ is the beampattern of FDA, and $\Psi_{\text{FDA}} = \text{angle}(E_{\text{FDA}})$ is the radiation phase pattern of FDA, with *angle* being the phase angle solving function.

2.2 Model of amplitude-comparison monopulse system

As shown in Fig. 2, the amplitude-comparison monopulse reconnaissance system distributes the N receivers with the same beampattern $F(\theta)$ evenly in all directions, so the angle of the adjacent receivers is $\theta_s = 2\pi/N$. Assuming that the starting receiver is positioned at azimuth θ_1 , then the direction of each receiver can be expressed as,

$$\theta_n = \theta_1 + (n-1)\theta_s \quad n = 1, 2, \dots, N \tag{6}$$

Then, the beampattern of each receiver can be given by

$$F_n(\theta) = F(\theta - \theta_n) \quad n = 1, 2, \dots, N \tag{7}$$

Figure 3 shows the direction-finding principle of the amplitude-comparison monopulse, the logarithmic envelope amplification of the signal received by the receivers through the receiving channel with an amplitude gain of k_n are

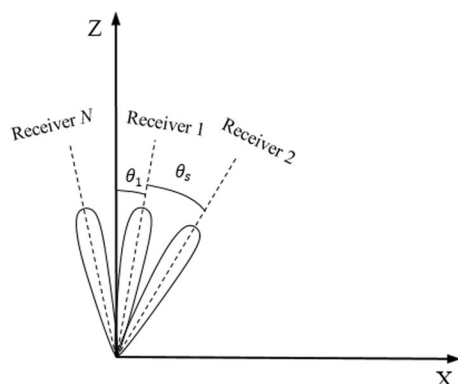


Fig. 2 The model of amplitude-comparison monopulse reconnaissance system

$$s_n(t, \theta) = 10 \log [k_n F(\theta - \theta_n) A(t)] \quad n = 1, 2, \dots, N \quad (8)$$

where $A(t)$ denotes the pulse envelope of the received signal. Then, the azimuth angle estimation $\hat{\theta}$ of the incoming signal can be obtained by the direction-finding signal processor. The current signal processing methods used by the signal processor mainly include adjacent amplitude comparison and omnidirectional amplitude comparison. In this paper, the method we consider is adjacent amplitude comparison.

According to the adjacent amplitude-comparison method, the two strongest outputs of the adjacent receivers are found by the direction-finding signal processor, and thus, the DOA of the incoming signal can be determined to be between the two adjacent receivers. Assuming that the two outputs obtained are $s_n(t, \theta)$ and $s_{n+1}(t, \theta)$, the output voltage difference is

$$u = s_n(t, \theta) - s_{n+1}(t, \theta) = 10 \log \frac{k_n F(\theta - \theta_n)}{k_{n+1} F(\theta - \theta_{n+1})} \quad (9)$$

When the amplitude response of the receiving branch is consistent, that is, $k_n = k_{n+1}$, the relationship between the voltage difference u and the signal arrival direction θ is

$$u = 10 \log \frac{F(\theta - \theta_n)}{F(\theta - \theta_{n+1})} \quad (10)$$

When the receiver is a horn antenna, its beampattern $F(\theta)$ is approximately considered as Gaussian function, assuming that its half-power beam width is $\theta_{0.5}$, therefore

$$F(\theta) = e^{-1.3863 \left(\frac{\theta}{\theta_{0.5}} \right)^2} \quad (11)$$

Combining (10) and (11), then

$$u = \frac{6(\theta_{n+1} - \theta_n)}{\theta_r^2} (\theta_{n+1} + \theta_n - 2\theta) = \frac{6\theta_s}{\theta_{0.5}^2} [2\theta_1 + (2n - 1)\theta_s - 2\theta] \quad (12)$$

Then, the DOA of the signal is estimated as

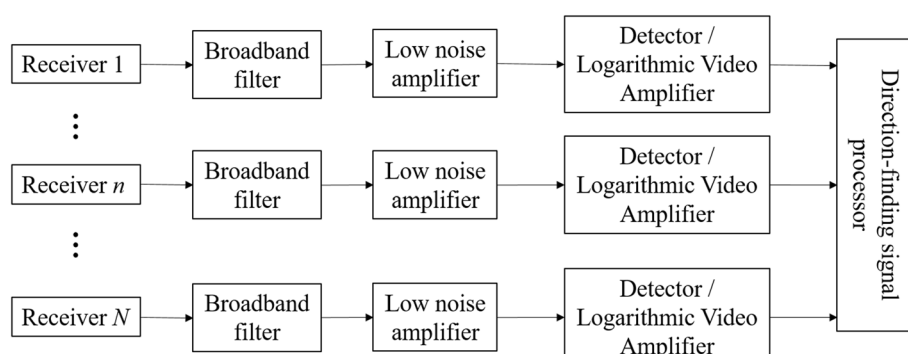


Fig. 3 Direction-finding principle of the amplitude-comparison monopulse

$$\hat{\theta} = \theta_1 + \left(n - \frac{1}{2} \right) \theta_s - \frac{\theta_{0.5}^2}{12\theta_s} u, \theta \in [\theta_n, \theta_{n+1}] \quad (13)$$

When the receiver is an array antenna, it is generally considered that its beampattern $F(\theta)$ is approximate to the Sinck function, assuming that its zero-power beam width is θ_0 , we have

$$F(\theta) = \frac{\sin\left(2\pi \frac{\theta}{\theta_0}\right)}{2\pi \frac{\theta}{\theta_0}} \quad (14)$$

Combining (10) and (14), then

$$\begin{aligned} u &= 10 \log \left[\frac{\sin\left(2\pi \frac{\theta-\theta_n}{\theta_0}\right)}{2\pi \frac{\theta-\theta_n}{\theta_0}} \right] - 10 \lg \left[\frac{\sin\left(2\pi \frac{\theta-\theta_{n+1}}{\theta_0}\right)}{2\pi \frac{\theta-\theta_{n+1}}{\theta_0}} \right] \\ &= 10 \log \left[\frac{(\theta - \theta_{n+1}) \sin\left(2\pi \frac{\theta-\theta_n}{\theta_0}\right)}{(\theta - \theta_n) \sin\left(2\pi \frac{\theta-\theta_{n+1}}{\theta_0}\right)} \right] \end{aligned} \quad (15)$$

Then, the DOA of the signal is estimated as

$$\hat{\theta} = \text{solve} \left\{ u = 10 \log \left[\frac{(\theta - \theta_{n+1}) \sin\left(2\pi \frac{\theta-\theta_n}{\theta_0}\right)}{(\theta - \theta_n) \sin\left(2\pi \frac{\theta-\theta_{n+1}}{\theta_0}\right)} \right], \theta \in [\theta_n, \theta_{n+1}] \right\} \quad (16)$$

where solve denotes the solving function.

3 Deception model of FDA against amplitude-comparison monopulse

Part 2.1 and 2.2 analyze the signal model of the FDA radar and the amplitude-comparison monopulse reconnaissance system, respectively. In practice, the amplitude-comparison monopulse direction-finding system distributes multiple receivers uniformly in the same position but in different directions. It determines the DOA of signals by comparing the amplitude of the signals received by different receivers. The incoming wave direction determined by the monopulse system is based on the received beampattern, which is affected by the frequency of the incoming wave. The above analysis is based on the fixed incoming wave frequency. However, according to the analysis in Part 2.1, we can know that by introducing a tiny frequency offset between adjacent elements, the FDA can achieve an S-shaped beampattern. Therefore, we can see that the FDA signal received by the direction-finding system does not conform to the direction-finding principle of the amplitude-comparison monopulse. Thus, the FDA may achieve the DOA location deception on the amplitude-comparison monopulse. To research the deception effect, we establish a DOA location deception model based on the FDA to contrast the amplitude-comparison monopulse direction-finding system.

3.1 Deception model based on FDA

Assuming that on arrival at the direction-finding system, the signal radiated by the FDA is with incidence angle θ , and the FDA radar and the amplitude-comparison

monopulse direction-finding system are in the same plane XOZ, then the position relationship between the direction-finding system and FDA radar is shown in Fig. 4.

Assuming that the receiver of the direction-finding system is an array antenna containing M elements, the signal received by the receiver n is

$$s_n(t, \theta) = \sum_{m=1}^M \sum_{q=1}^Q S_{lqm}(t) = \sum_{m=1}^M \sum_{q=1}^Q A_q A_m \exp [j2\pi f_q(t - R_{nqm}/c)] \quad (17)$$

where R_{nqm} is the range between element q of the FDA and element m of the receiver n , i.e.,

$$R_{nqm} = R - (q - 1)d \sin \theta + (m - 1)d_1 \sin (\theta - \theta_n) \quad (18)$$

Then, (17) can be further rewritten as

$$\begin{aligned} s_n(t, \theta) &= \sum_{m=1}^M \sum_{q=1}^Q A_q A_m \exp \left\{ j2\pi f_q \left[t - \left[\frac{R - (q - 1)d \sin \theta}{c} + (m - 1)d_1 \sin (\theta - \theta_n) \right] \right] \right\} \\ &= \sum_{m=1}^M \sum_{q=1}^Q A_q A_m \exp \left\{ j2\pi (f_0 + \Delta f_q) \left[t - \left[\frac{R - (q - 1)d \sin \theta}{c} + (m - 1)d_1 \sin (\theta - \theta_n) \right] \right] \right\} \end{aligned} \quad (19)$$

Assuming that the amplitude of the radiated signal of each transmitting element and the receiving gain of the receiving element are both considered to be equal, i.e. $A_q = A = 1$, $A_m = A = 1$, (19) can be rewritten as

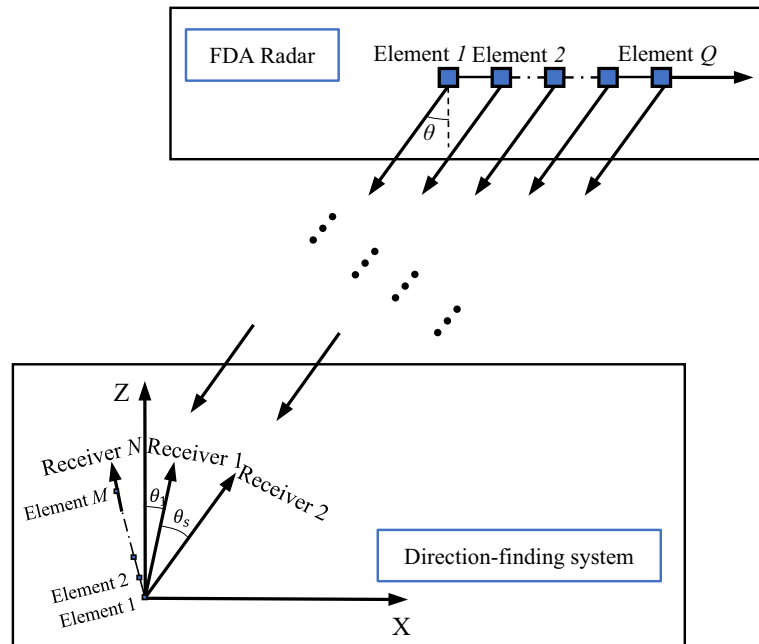


Fig. 4 The position relationship between the direction-finding system and FDA radar

$$\begin{aligned}
s_n(t, \theta) &= \sum_{m=1}^M \sum_{q=1}^Q \exp \left\{ j2\pi(f_0 + \Delta f_q) \left[t - \frac{R - (q-1)d \sin \theta + (m-1)d_1 \sin(\theta - \theta_n)}{c} \right] \right\} \\
&= \sum_{q=1}^Q \sum_{m=1}^M \exp \left\{ j2\pi(f_0 + \Delta f_q) \left[t - \frac{R - (q-1)d \sin \theta + (m-1)d_1 \sin(\theta - \theta_n)}{c} \right] \right\} \\
&= \sum_{q=1}^Q \frac{\sin(M\pi(f_0 + \Delta f_q)d_1 \sin(\theta - \theta_n))}{\sin(\pi(f_0 + \Delta f_q)d_1 \sin(\theta - \theta_n))} \\
&\quad \exp \left\{ j2\pi(f_0 + \Delta f_q) \left[t - \frac{R - (q-1)d \sin \theta + (M-1)d_1 \sin(\theta - \theta_n)/2}{c} \right] \right\}
\end{aligned} \tag{20}$$

For the phased array signal, i.e. $\Delta f_q = 0$, then

$$s_{PA_n}(t, \theta) = \exp \left\{ j\phi_1 \right\} \frac{\sin[M\pi f_0 d_1 \sin(\theta - \theta_n)]}{\sin[\pi f_0 d_1 \sin(\theta - \theta_n)]} \frac{\sin(Q\pi f_0 d \sin \theta)}{\sin(\pi f_0 d \sin \theta)} \tag{21}$$

$$\text{where } \phi_1 = 2\pi f_0 \left\{ t - \left[\frac{R - (Q-1)d \sin \theta / 2}{c} + \frac{(M-1)d_1 \sin(\theta - \theta_n) / 2}{c} \right] \right\}.$$

Combining (20) and (21), we learn that compared with phased array signal, the amplitude of the FDA signal received by the amplitude-comparison monopulse direction-finding system is coupled with distance, time and angle, due to the introduction of the small frequency offset among the elements. Therefore, the direction-finding system cannot accurately estimate the DOA of the signal. In fact, assuming that the outputs of direction-finding signal processor are $s_n(t, \theta)$ and $s_{n+1}(t, \theta)$, the signal can be determined to be between the included angle of the two adjacent receivers. Then, the estimated DOA obtained by the direction-finding system is

$$\hat{\theta} = \text{solve} \left[\frac{s_n(t, \theta)}{s_{n+1}(t, \theta)} = \frac{\sin[\pi f_0 d_1 \sin(\theta - \theta_{n+1})]}{\sin[M\pi f_0 d_1 \sin(\theta - \theta_{n+1})]} \cdot \frac{\sin[M\pi f_0 d_1 \sin(\theta - \theta_n)]}{\sin[\pi f_0 d_1 \sin(\theta - \theta_n)]}, \theta \in [\theta_n, \theta_{n+1}] \right] \tag{22}$$

And the location estimation can be expressed as

$$\hat{x} = R \sin \hat{\theta} \tag{23}$$

The location deviation is

$$\Delta x = R \sin \hat{\theta} - R \sin \theta \tag{24}$$

Generally, when the measured location deviates from the transmitting antenna array, the deception effect on the direction-finding system is considered better, i.e.

$$\Delta x > 0 \quad \text{or} \quad \Delta x < -(Q-1)d \tag{25}$$

3.2 Model verification and performance analysis

3.2.1 SNR analysis

Signal-to-noise ratio (SNR) is an important parameter in the direction-finding system. As the analyses above, we can know that the FDA can generate a range-angle-time-dependent beampattern. Thus, in the constant noise environment, the FDA

signal has the time-varying SNR, while the PA signal has the approximately constant SNR. Therefore, we define the instantaneous SNR (ISNR) to express the time-varying SNR:

$$\text{ISNR}_{\text{FDA}}(t) = 10 \log \left(\frac{P_{\text{FDA}}(t)}{P_w} \right) \quad (26)$$

where $P_w = w_0 B$ denotes the average power of noise, with w_0 and B being the unilateral power spectral density of noise and the bandwidth of FDA signal, respectively. Besides the FDA signal power $P_{\text{FDA}}(t)$ can be given by

$$P_{\text{FDA}}(t) = \frac{1}{\tau} \int_t^{t+\tau} |E_{\text{FDA}}(t)|^2 dt = \frac{1}{\tau} \int_t^{t+\tau} |A_{\text{BP_FDA}}(t)|^2 dt \quad (27)$$

where t and τ denotes the starting time and period of sampling, respectively.

The SNR of PA can be then given by,

$$\text{SNR}_{\text{PA}} = \text{ISNR}_{\text{PA}}(t) = 10 \log \left(\frac{P_{\text{PA}}}{P_w} \right) \quad (28)$$

where

$$P_{\text{PA}} = |E_{\text{PA}}|^2 = |A_{\text{BP_PA}}|^2 = |A_{\text{BP_FDA}}(t)|_{\Delta f_{1:Q}=0}^2 \quad (29)$$

As the analysis above, the SNR is mainly affected by the antenna gain of the different signals. Therefore, for the fixed far-field target, the antenna gain ratio of the FDA to the PA can be expressed as

$$h(t) = \frac{|E_{\text{FDA}}(t)|}{|E_{\text{PA}}|} = \frac{|E_{\text{FDA}}(t)|}{|E_{\text{FDA}}(t)|_{\Delta f_{1:Q}=0}} = \frac{|A_{\text{BP_FDA}}(t)|}{|A_{\text{BP_FDA}}(t)|_{\Delta f_{1:Q}=0}} \quad (30)$$

Following the same signal-arriving-time assumption, it holds that $|E_{\text{PA}}| = |E_{\text{FDA}}(t)|_{\Delta f_{1:Q}=0} = \max |E_{\text{FDA}}(t)|$, i.e.,

$$h(t) = \frac{|E_{\text{FDA}}(t)|}{\max |E_{\text{FDA}}(t)|} \leq 1 \quad (31)$$

Therefore, following the same noise environment and signal-arriving time assumption, the ISNR of the FDA signal will not exceed the SNR of the PA signal.

3.2.2 Error analysis

Positioning error is an important parameter to describe the positioning accuracy of the direction-finding system. However, one of the primary objectives of our deception method is to increase the measurement error of the direction-finding system. Therefore, to indicate the superiority of our deception method, the root-mean-square error (RMSE) and variation (Var) are derived.

Under the condition of Monte Carlo experiments, the RMSE of angle measurement $\hat{\theta}$ is given by

$$\text{RMSE}(\hat{\theta}) = \sqrt{E[(\hat{\theta} - \theta)^2]} = \sqrt{\text{Var}(\hat{\theta}) + [E(\hat{\theta}) - \theta]^2} \quad (32)$$

where $\text{Var}(\hat{\theta})$ represents the variance of $\hat{\theta}$, and it can be calculated as

$$\text{Var}(\hat{\theta}) = E\left\{[\hat{\theta} - E(\hat{\theta})]^2\right\} \quad (33)$$

Similar to (32), the RMSE of \hat{x} can be also given by

$$\text{RMSE}(\hat{x}) = \sqrt{E[(\hat{x} - x)^2]} = \sqrt{\text{Var}(\hat{x}) + [E(\hat{x}) - x]^2} \quad (34)$$

where $\text{Var}(\hat{x}) = E\{[\hat{x} - E(\hat{x})]^2\}$ denotes the variance of \hat{x} .

Actually, since the array antenna cannot be considered as a point, we generally take the array center into consideration, let $\hat{x}_0 = R \sin \hat{\theta}$ and $x_0 = x - (Q - 1)d/2$, we have,

$$\text{RMSE}(\hat{x}_0) = \sqrt{E[(\hat{x}_0 - x_0)^2]} = \sqrt{\text{Var}(\hat{x}_0) + [E(\hat{x}_0) - x_0]^2} \quad (35)$$

where $\text{Var}(\hat{x}) = \text{Var}(\hat{x}_0)$.

3.2.3 CRLB analysis

Cramér–Rao Lower Bound (CRLB) shows the ideal performance that the direction-finding system can achieve. However, different signals actually have different characteristics, meaning that the different signals the system receives, the different performances are. In other words, if the FDA signals have the higher CRLB than other deceptive signals, the FDA signals have a better deception effect. Suppose $A_{\text{FDA}}(t)$ is the transmit beam of the FDA, then we have

$$\begin{aligned} s_n(t, \theta) &\approx A_{\text{FDA}}(t) \frac{\sin[M\pi f_0 d_1 \sin(\theta - \theta_n)]}{\sin[\pi f_0 d_1 \sin(\theta - \theta_n)]} \\ &\quad \exp\left\{j\pi f_0 \left[2t - \frac{2R - (Q - 1)d \sin \theta + (M - 1)d_1 \sin(\theta - \theta_n)}{c}\right]\right\} \\ &= A_{\text{FDA}}(t) A_r(\theta) \exp\left\{j\pi f_0 \left[2t - \frac{2R - (Q - 1)d \sin \theta + (M - 1)d_1 \sin(\theta - \theta_n)}{c}\right]\right\} \\ &\approx A_{\text{FDA}}(t) A_r(\theta) \exp\left\{j\pi f_0 \left[2t - \frac{2R - (Q - 1)d \sin \theta + (M - 1)d_1(\theta - \theta_n)}{c}\right]\right\} \\ &= A_{\text{FDA}}(t) A_r(\theta) \exp\{j(\phi \theta_n + \psi)\} \end{aligned} \quad (36)$$

where

$$A_r(\theta) = \frac{\sin[M\pi f_0 d_1 \sin(\theta - \theta_n)]}{\sin[\pi f_0 d_1 \sin(\theta - \theta_n)]} \quad (37-1)$$

$$\phi = \pi f_0(M - 1)d_1/c \quad (37-2)$$

$$\psi = 2\pi f_0(t - R/c) + \pi f_0[(Q-1)d \sin \theta / c - (M-1)d_1 \theta / c] \quad (37-3)$$

Then, the general signal sampling processed by the N -receiver monopulse direction-finding system can be expressed as

$$\begin{aligned} \mathbf{x}[n] &= \mathbf{s}[n] + \mathbf{w}[n] \\ &= |A(t, \theta)| \exp(j(\phi \theta_n + \psi)) + \mathbf{w}[n] \quad n = 0, 1, \dots, N-1 \end{aligned} \quad (38)$$

where $A(t, \theta) = A_{\text{FDA}}(t)A_r(\theta)$ denotes the received signal amplitude.

Therefore, the CRLBs of the FDA signals for the measured DOA and location error are

$$\text{CRLB}_{\text{FDA-}\theta} = \frac{\tan^2 \theta}{2N \cdot \text{ISNR}_{\text{FDA}} \cdot [M \cos(M\varphi) - A_r(\theta)]^2} \quad (39-1)$$

$$\text{CRLB}_{\text{FDA-}x} = \frac{R^2 \sin^2 \theta}{2N \cdot \text{ISNR}_{\text{FDA}} \cdot [M \cos(M\varphi) - A_r(\theta)]^2} \quad (39-2)$$

Similarly, the CRLB of PA signals is derived by

$$\text{CRLB}_{\text{PA-}\theta} = \frac{\tan^2 \theta}{2N \cdot \text{SNR}_{\text{PA}} \cdot [M \cos(M\varphi) - A_r(\theta)]^2} \quad (40-1)$$

$$\text{CRLB}_{\text{PA-}x} = \frac{R^2 \sin^2 \theta}{2N \cdot \text{SNR}_{\text{PA}} \cdot [M \cos(M\varphi) - A_r(\theta)]^2} \quad (40-2)$$

As the analysis above, we can know following the same noise environment and signal-arriving time assumption, the ISNR of the FDA do not exceed that of the PA, meaning that $\text{CRLB}_{\text{FDA}} \geq \text{CRLB}_{\text{PA}}$, i.e., the FDA signals have a better deception effect than the PA signals.

4 Experiment results and discussion

To investigate the deception effect of the FDA signals, the non-noise and Gaussian white noise environments are taken into consideration. Meanwhile, as we know that the beam of FDA varies over time, so the influence of time is also verified. So, for the adjacent amplitude-comparison monopulse direction-finding system, the simulation settings and the representative antenna linear arrays are given in Tables 1 and 2, respectively.

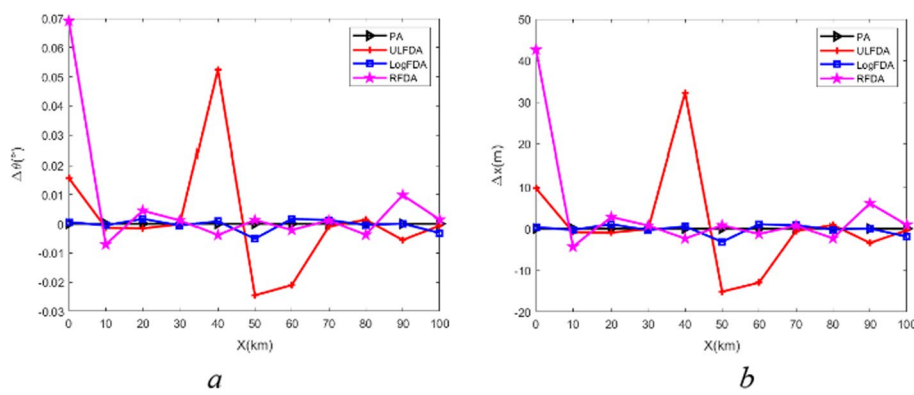
Example 1: Deception effect with no noise and fixed time: inspired by the signal model of FDA, we know that the FDA can generate a range-dependent beampattern because of its small frequency increment. Moreover, by analyzing the proposed deception model, we know that the FDA mainly achieves deception on the amplitude-comparison monopulse by its unique beampattern. Hence, while setting $z = 25\sqrt{2}$ km, Fig. 5 gives the estimation error with x . Figure 5a shows the DOA deviation change with x ; we can see with the increase in x , the DOA deviation of PA is nearly unchanged while those of ULFDA and RFDA change sharply. Besides, the DOA deviation of Log-FDA shows a slight change. Figure 5b shows the location deviation change with x ; we can see that there is the same trend for the location deviation with x changing. For

Table 1 Simulation settings

Names	Symbols	Settings
Carrier frequency	f_0	1 GHz
Array frequency increment	Δf	100 kHz
Number of array elements	Q	10
Element spacing of radar array	d	0.15 m
Number of receivers	N	72
The angle of the adjacent antennas	θ_s	5°
The azimuth of the first receiver	θ_1	0°
Number of the monopulse antenna elements	M	10
Array element spacing of the monopulse antenna array	d_1	0.15 m
Incident angle	θ	45°
The range from FDA to the receiver	R	50 km
The x-axis coordinates from receiver1 to radar	x	$25\sqrt{2}$ km
The z-axis coordinates from receiver1 to radar	z	$25\sqrt{2}$ km

Table 2 Representative antenna linear arrays

Array structures	Frequency increment sequence
Phased array (PA)	$\Delta f \cdot \underbrace{[0 \ 0 \ \dots \ 0 \ \dots \ 0]}_Q$
Uniform linear FDA (ULFDA)	$\Delta f \cdot \underbrace{[0 \ 1 \ \dots \ q-1 \ \dots \ Q-1]}_Q$
Linear FDA with Log variation frequency increment (LogFDA)	$\Delta f \cdot \underbrace{[0 \ \log(2) \ \dots \ \log(q) \ \dots \ \log(Q)]}_Q$
Linear FDA with random frequency increment (RFDA)	$\Delta f \cdot \underbrace{[0 \ \text{rand}(Q) \ \dots \ \text{rand}(Q) \ \dots \ \text{rand}(Q)]}_Q$

**Fig. 5** Estimation error with x . **a** DOA estimation and **b** Location estimation

PA, we know that the estimation location does not exceed the antenna array, while those of the FDAs exceed the antenna array. The changes in Fig. 5 indicate that with the change of x , the amplitude-comparison monopulse system can estimate the DOA

and the location of the PA signal accurately, without being able to do so on the FDA signals. Fixing the receivers at $(25\sqrt{2} \text{ km}, 25\sqrt{2} \text{ km})$, Fig. 6 gives the estimation error with Δf . Figure 6a shows the DOA deviation change with Δf ; it can be seen that with the increase in Δf , the DOA deviation of PA is almost unchanged while those of ULFDA, RFDA and LogFDA show a change; among them, the DOA deviation of ULFDA changes sharply. Figure 6b shows the location deviation change with Δf ; we can see that there is the same trend for the location deviation. Besides, for PA, we can know that the estimation location does not exceed the antenna array with Δf changing, while those of the FDAs exceed the antenna array. Figure 6 shows that the FDA can achieve better DOA location deception by choosing the appropriate frequency increment. Combining the results of Figs. 5 and 6, we know that the FDA signals have the deception effect on the amplitude-comparison monopulse direction-finding system.

Example 2: Deception effect with no noise and varying time: actually, the beampattern of FDA is also time-dependent, meaning that the influence of time should be considered. Following non-noise assumption, Fig. 7 gives the estimation error with t . Figure 7a shows the DOA estimation error with t ; we can see with the increase in t ; the $\Delta\theta$ of PA and ULFDA hardly change. But differently, the $\Delta\theta$ of ULFDA remains in a certain degree of change while that of PA is nearly 0. Meanwhile, the $\Delta\theta$ of LogFDA and RFDA show dramatic changes, especially that of RFDA. Figure 7b shows the Δx with t , and there is a same trend as $\Delta\theta$. For PA, we can know that the estimation location does not exceed the antenna array, while that of the ULFDA do exceed the antenna array. Nevertheless, for LogFDA and RFDA, the location deviations change dramatically along the antenna array, which is also tricky for direction-finding system to locate the antenna arrays over the observation time. In general, the FDAs can realize DOA location deception against the amplitude-comparison monopulse direction-finding system during the observation time.

Example 3: Deception effect with Gaussian white noise and fixed time: as we know, the processes of transmitting and receiving signals expose in the noisy environment, so it is necessary to investigate the deception effect of the FDA in the noisy environment. Therefore, following the same Gaussian white noise assumption, taking the

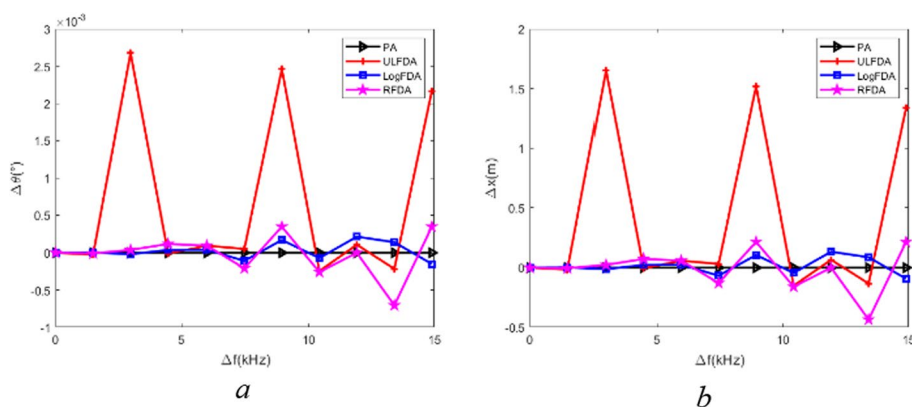


Fig. 6 Estimation error with Δf . **a** DOA estimation and **b** Location estimation

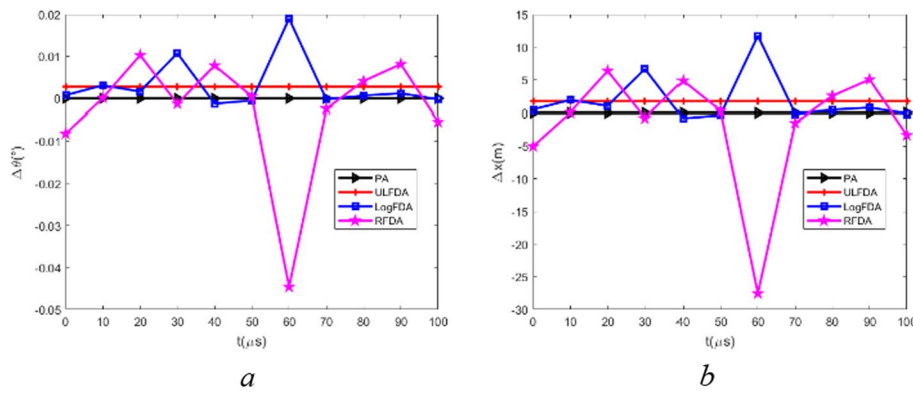


Fig. 7 Estimation error with t . **a** DOA estimation and **b** Location estimation

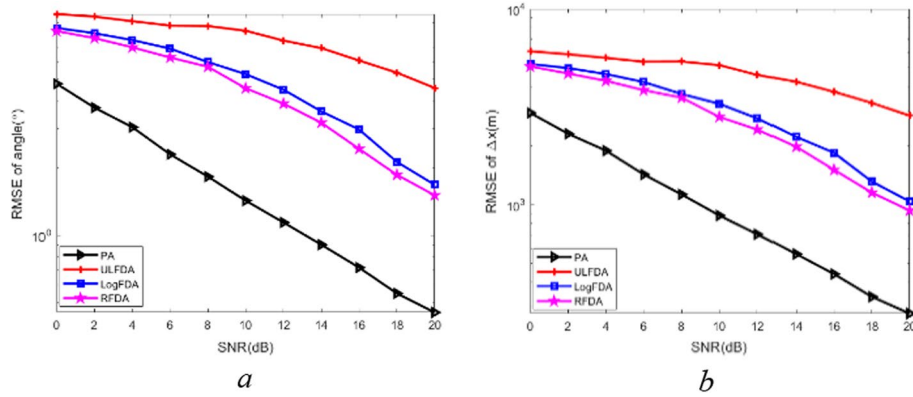


Fig. 8 Estimation RMSE with SNR. **a** DOA RMSE and **b** Location RMSE

SNR of PA as a reference, and fixing $t = 20 \mu\text{s}$, Fig. 8 shows the estimation RMSE with SNR through 5000 Monte Carlo experiments. We find that with the increase in SNR, the RMSE of ULFDA shows the most significant deviation and the lowest reduction rate, while PA does the opposite. Taking 2000 Monte Carlo experiments and setting $t = 20 \mu\text{s}$, Fig. 9 shows the estimation error with SNR. The DOA and location Vars of the four structures are always higher than their corresponding CRLB. And as the analysis in Section III, the higher the CRLB, the better the deception effect of the FDA signals. Therefore, from Fig. 9, we can see that the ULFDA has the highest deception effect on the direction-finding system. Combining the results of Figs. 8 and 9, it can be seen that when fixing time, the FDA signals have the deception effect on the amplitude-comparison monopulse direction-finding system under the noise environment.

Example 4: Deception effect with Gaussian white noise and varying time: for the amplitude-comparison monopulse direction-finding system, the DOA location process is time-dependent, so it is necessary to explore the effect of time on deception in the noise environment. Therefore, through 5000 Monte Carlo experiments, Fig. 10 shows the CRLB and Beampattern with t . We can see that the FDAs have a larger CRLB than the PA, while the CRLBs of LogFDA and RFDA change sharply. Moreover, comparing Fig. 10c with (a) and (b), it can be seen that the CRLB shows an

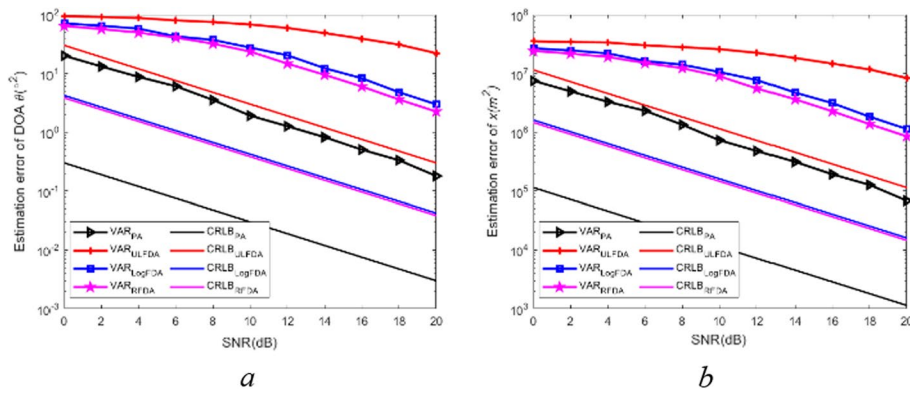


Fig. 9 Estimation error with SNR. **a** DOA estimation and **b** Location estimation

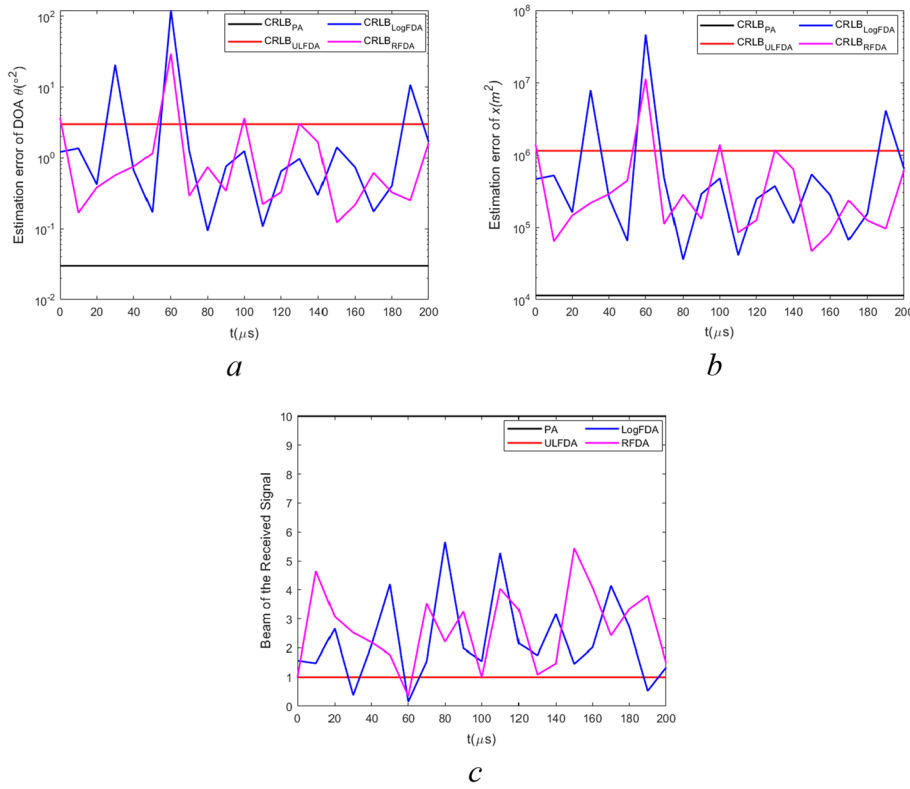


Fig. 10 CRLB and Beampattern with t . **a** DOA CRLB, **b** Location CRLB, and **c** Beampattern

opposite trend to the beampattern. Figure 11 gives the estimation error with t while $\text{SNR} = 10 \text{ dB}$. Similar to the analysis of *Example 3*, the higher the CRLB, the better the deception effect of the FDA signals. Therefore, we can see that the LogFDA and RFDA have higher deception effects on the amplitude-comparison monopulse direction-finding system, while the ULFDA has a more stable deception effect. Combining the results of Figs. 10 and 11, we can see that the FDA signal has the deception effect on the amplitude-comparison monopulse direction-finding system under the noisy and time-varying observation.

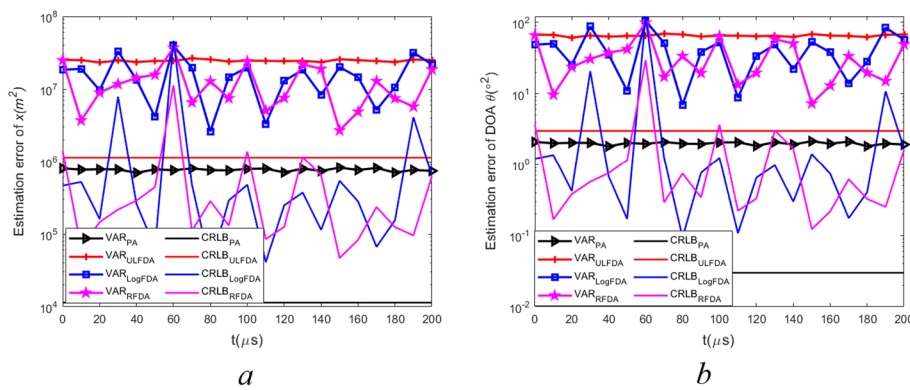


Fig. 11 Estimation error with t . **a** DOA estimation and **b** Location estimation

5 Conclusion

The FDA shows feasibility in counteracting the monopulse direction-finding system as its angle-range-time-dependent beampattern. Therefore, we have studied the deception effect of the FDAs against the amplitude-comparison monopulse direction-finding system. The theoretical and mathematical analysis shows that, by introducing the frequency increment around the elements, the FDA can generate signals that do not conform to the direction-finding principle of the amplitude-comparison monopulse. After that, we establish the deception model for the FDA signals to counteract the amplitude-comparison monopulse direction-finding system. Furthermore, to verify the performance of the proposed deception model, the ISNR, MESE, Var, and CRLB are derived mathematically. Numerical examples and simulations show: (1) Without considering the influence of the noise, the FDA signals have the deception effect on the amplitude-comparison monopulse direction-finding system, and the deception effects are varied with the observation time. (2) While in the Gaussian white noise environment, the FDA signals can also counteract the amplitude-comparison monopulse direction-finding system, both for the case of fixed and varying time. In future work, we will concentrate on configuring the FDA signals to get the ideal deception effect, based on which the amplitude-comparison monopulse system can do little harm on our radar.

Abbreviations

FDA	Frequency diversity array
PA	Phased array
ULFDA	Uniform linear FDA
LogFDA	Linear FDA with Log variation frequency increment
RFDA	Linear FDA with random frequency increment
DOA	Direction-of-arrival
ISNR	Instantaneous signal-to-noise ratio
CRLB	Cramér–Rao lower bound
RMSE	Root-means-square error
Var	Variation
PAR	Phased array radar
LPI	Low probability of interception
ECMS	Electronic countermeasures
RF	Radio frequency

Acknowledgements

The authors would like to thank the anonymous reviewers for their valuable comments and suggestions that helped improve the quality of the manuscript.

Author contributions

JG contributed to conceptualization, formal analysis, methodology, resources, validation, and writing—original draft; JX contributed to formal analysis, supervision, and writing—review and editing. Both authors read and approved the final manuscript.

Authors' information

Ge Jiaang, was born in 1995 and received the bachelor degree from BeiHang University, Beijing, the People's Republic of China (PRC), in 2017. He is currently a doctoral student in the Air and Missile Defense College, Air Force Engineering University, Shaanxi, Xi'an, the People's Republic of China (PRC). His research interest is radar signal processing, electronic countermeasures (ECMS) and active anti-jamming.

Xie Junwei, was born in 1970 and received the bachelor, master, and doctor degrees from the Air and Missile Defense College, Air Force Engineering University, Shaanxi, Xi'an, the People's Republic of China (PRC), in 1993, 1996, 2009, respectively. He is currently a professor in the Air and Missile Defense College. His research interests include novel radar systems as well as jamming and anti-jamming. Pro. Xie has published more than 100 refereed journal articles, book chapters, and conference papers.

Funding

Not applicable.

Availability of data and materials

The datasets generated during the current study are not publicly available but are available from the corresponding author on reasonable request.

Declarations

Ethics approval and consent to participate

Not applicable.

Consent for publication

Not applicable.

Competing interests

The authors declare that they have no competing interests.

Received: 22 March 2022 Accepted: 14 June 2022

Published online: 28 June 2022

References

1. G. Liu, et al., The analysis and design of modern low probability of intercept radar, in *2001 CIE International Conference on Radar Proceedings* (Cat No.01TH8559) (2001), pp. 120–124
2. W. Qianzhe et al., Overview on RF stealth technology research. *J. Electron. Inf. Technol.* **40**(6), 1505–1514 (2018)
3. D.C. Schleher, LPI radar: fact or fiction. *IEEE Aerosp. Electron. Syst. Mag.* **21**(5), 3–6 (2006)
4. R.C. Hansen, *Phased Array Antennas* (2009)
5. J. Zheng, R. Chen, T. Yang, X. Liu et al., An Efficient strategy for accurate detection and localization of UAV swarms. *IEEE Internet Things J.* **20**(8), 15372–15381 (2021)
6. J. Zheng, T. Yang, H. Liu, T. Su et al., Accurate detection and localization of UAV swarms-enabled MEC system. *IEEE Trans. Ind. Inf.* **17**(7), 5059–5067 (2021)
7. R.J. Mailloux, *Phased Array Antenna Handbook* (Artech House, London, 1993)
8. M.P. Daly, J.T. Bernhard, Directional modulation technique for phased arrays. *IEEE Trans. Antennas Propag.* **57**(9), 2633–2640 (2009)
9. L. Bao et al., Influence of blinking jamming of dual stealth aircraft on the performance of monopulse radar. *J. Syst. Eng. Electron.* **42**(3), 589–596 (2020)
10. X. Geng, et al., The influence of synchronous blinking jamming on monopulse radar seeker angular resolution, in *International Conference on Logistics Engineering, Management and Computer Science* (LEMCS 2015) (2015), pp. 226–229
11. K. Davidson, J. Bray, Theory and design of blink jamming. *Appl. Sci.* **10**(6), 1914 (2020)
12. H. Han, et al., Analysis of cross-polarization jamming for phase comparison monopulse radars, in *2019 IEEE 2nd International Conference on Electronic Information and Communication Technology* (ICEICT) (2019)
13. I. Kalinbacak, et al., Cross polarization monopulse jammer located on UAV, in *2017 8th International Conference on Recent Advances in Space Technologies* (RAST) (2017), pp. 337–341
14. C. Xingjian, Simulation and analysis of cross-polarization monopulse radar angle deception jamming. *Electron. Sci. Technol.* **26**(10), 131–132, 144 (2013)
15. W.P. Du Plessis, Platform skin return and retrodirective cross-eye jamming. *IEEE Trans. Aerosp. Electron. Syst.* **48**(1), 490–501 (2012)
16. W.P. du Plessis et al., Tolerance analysis of cross-eye jamming systems. *IEEE Trans. Aerosp. Electron. Syst.* **47**(1), 740–745 (2011)
17. T. Liu et al., Performance analysis of multiple-element retrodirective cross-eye jamming based on linear array. *IEEE Trans. Aerosp. Electron. Syst.* **51**(3), 1867–1876 (2015)
18. P. Antonik, M.C. Wicks, H.D. Griffiths, C.J. Baker, Frequency diverse array radars, in *IEEE Conference on Radar* (2006)

19. Y. Xu, X. Shi, J. Xu, P. Li, Range-angle-dependent beamforming of pulsed frequency diverse array. *IEEE Trans. Antennas Propag.* **63**(7), 3262–3267 (2015)
20. H. Chen, H. Shao, H. Chen, Angle-range-polarization-dependent beamforming for polarization sensitive frequency diverse array. *EURASIP J. Adv. Signal Process.* **1**, 2019 (2019)
21. J. Xu, G. Liao, S. Zhu, L. Huang, H.C. So, Joint range and angle estimation using MIMO radar with frequency diverse array. *IEEE Trans. Signal Process.* **63**(13), 3396–3410 (2015)
22. C. Wang et al., FDA-MIMO for joint angle and range estimation: unfolded coprime framework and parameter estimation algorithm. *IET Radar Sonar Navig.* **14**(6), 917–926 (2020)
23. L. Huang et al., Joint range and angle estimation based on sub-array scheme with frequency diverse array radar. *Int. J. Electron. Electr. Eng.* (2017). <https://doi.org/10.18178/ijeee.5.1.30-34>
24. B. Li, W. Bai, Q. Zhang, G. Zheng, The polarization sensitive FDA-MIMO radar: performance analysis of beamforming based on oblique projection. *J. Phys.: Conf. Ser.* **1168**, 032119 (2019)
25. X. Li, D. Wang, X. Ma, W. Wang, Three-dimensional target localization method based on the tensor subspace FDS-MIMO radar with a co-prime frequency offset. *Sci. Sin. Inform.* **49**(1), 87–103 (2019)
26. W.-Q. Wang, Adaptive RF stealth beamforming for frequency diverse array radar, in *2015 23rd European Signal Processing Conference (EUSIPCO)* (2015), pp. 1158–1161
27. J. Xiong et al., "Cognitive FDA-MIMO radar for LPI transmit beamforming. *IET Radar Sonar Navig.* **11**(10), 1574–1580 (2017)
28. J. Ge et al., A cognitive active anti-jamming method based on frequency diverse array radar phase center. *Digit. Signal Process.* **109**, 102915 (2021)
29. J. Ge et al., The DOA location deception effect of frequency diverse array on interferometer. *IET Radar Sonar Navig.* **15**(3), 294–309 (2021)
30. X. Zhang et al., On RF localisation deception capability of FDA signal under interferometry reconnaissance. *J. Eng.* **2019**(20), 6695–6698 (2019)
31. Y. Hou, W.-Q. Wang, Active frequency diverse array counteracting interferometry-based DOA reconnaissance. *IEEE Antennas Wirel. Propag. Lett.* **18**(9), 1922–1925 (2019)
32. L. Wang, et al., On FDA RF localization deception under sum difference beam reconnaissance, in *2018 IEEE Radar Conference (RadarConf18)* (2018), pp. 269–273

Publisher's Note

Springer Nature remains neutral with regard to jurisdictional claims in published maps and institutional affiliations.

Submit your manuscript to a SpringerOpen® journal and benefit from:

- Convenient online submission
- Rigorous peer review
- Open access: articles freely available online
- High visibility within the field
- Retaining the copyright to your article

Submit your next manuscript at ► springeropen.com